

**Atomic layer deposition for membrane interface engineering**

Journal:	<i>Nanoscale</i>
Manuscript ID	NR-MRV-10-2018-008114.R1
Article Type:	Minireview
Date Submitted by the Author:	29-Oct-2018
Complete List of Authors:	Yang, Hao-Cheng; Sun Yat-sen University, School of Chemical Engineering and Technology Waldman, Ruben; University of Chicago, Institute for Molecular Engineering Chen, Zhaowei; Argonne National Laboratory, Center for Nanoscale Materials Darling, Seth; Argonne National Laboratory, Institute for Molecular Engineering; Argonne National Laboratory, Chemical Sciences & Engineering Division; Argonne National Laboratory, Advanced Materials for Energy-Water Systems Center; University of Chicago, Institute for Molecular Engineering

## Atomic layer deposition for membrane interface engineering

Hao-Cheng Yang<sup>a</sup>, Ruben Z. Waldman<sup>bc</sup>, Zhaowei Chen<sup>d</sup>, and Seth B. Darling<sup>\*bcef</sup>

Received 00th January 20xx,  
Accepted 00th January 20xx

DOI: 10.1039/x0xx00000x

www.rsc.org/

In many applications, interfaces govern the performance of membranes. Structure, chemistry, electrostatics, and other properties of interfaces can dominate the selectivity, flux, fouling resistance, and other critical aspects of membrane functionality. Control over membrane interfacial properties, therefore, is a powerful means of tailoring performance. In this minireview, we discuss the application of atomic layer deposition (ALD) and related techniques in the design of novel membrane interfaces. We discuss recent literature in which ALD is used to 1) modify the surface chemistry and interfacial properties of membranes, 2) tailor the pore sizes and separation characteristics of membranes, and 3) enable novel advanced functional membranes.

### 1. Introduction

Water stress—and its interrelation with energy—is a burgeoning societal concern, and new methods for efficiently and effectively purifying water are of critical importance. Membrane technologies are of particular interest in tackling water crises owing to their comparative advantages of low energy consumption and high separation efficiency.<sup>1–3</sup> The membrane surface plays a crucial role during separation processes because it directly contacts and interacts with the filtrating medium.<sup>4,5</sup> Membrane interface engineering is a physical or chemical process to tailor the surface properties of a membrane to enhance performance or even to impart novel functionality. Numerous surface modification strategies, including plasma treatment,<sup>6,7</sup> dip-/spin-coating,<sup>8</sup> surface grafting,<sup>9,10</sup> interfacial assembly,<sup>11,12</sup> surface deposition,<sup>13,14</sup> among others,<sup>15</sup> have been developed. These conventional methods often face a variety of challenges such as poor stability, damage to membrane structure, limited applicable substrates, and non-uniform modification. Polyolefins and fluoropolymers, such as polyethylene (PE), polypropylene (PP), polytetrafluoroethylene (PTFE), and polyvinylidene fluoride (PVDF), are the most prevalent materials for commercial membranes owing to their good mechanical strength and chemical stability. Most of the physical and chemical approaches listed above are unable to successfully modify these membranes because of their low-energy surface and inert

chemical structure. On the other hand, surface modification with inorganic components offers an alternative pathway to membrane interface engineering, in particular (but not exclusively) for polymer membranes.<sup>16</sup> Such strategies combine the advantages of both organic and inorganic materials and can introduce novel properties and functionality (e.g. catalytic, anti-bacterial, and adsorptive activities) to the membrane surface. Compared with grafting organic components, integrating inorganic components with polymer membranes is more challenging due to the poor interfacial compatibility between the two components, and a pre-modification step is often required to enhance the interactions between the membrane surface and the inorganic components, which complicates the modification process.

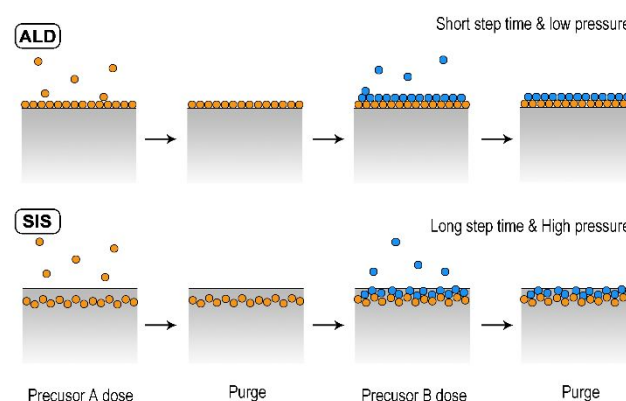


**Figure 1.** Schematic illustration of atomic layer deposition (ALD) and sequential infiltration synthesis (SIS) processes.

**Atomic layer deposition (ALD) is a process by which alternating surface-limiting exposures of reactant vapors enable layer-by-layer growth of materials such as metal oxides, metals, and even organic materials (Fig. 1, top).**<sup>17,18</sup> In a typical ALD cycle, the substrate is put in a near-vacuum chamber filled with inert gas (i.e. N<sub>2</sub>, Ar), and precursor vapors carried by inert gas are alternatively pulsed into the chamber. An atomic layer

<sup>a</sup> School of Chemical Engineering and Technology, Sun Yat-Sen University, Zhuhai, 519082, China

<sup>b</sup> Institute for Molecular Engineering, University of Chicago, Chicago, IL 60637, USA

<sup>c</sup> Chemical Sciences and Engineering Division, Argonne National Laboratory, Lemont, IL 60439, USA

<sup>d</sup> Center for Nanoscale Materials, Argonne National Laboratory, Lemont, IL 60439, USA

<sup>e</sup> Institute for Molecular Engineering, Argonne National Laboratory, Lemont, IL 60439, USA

<sup>f</sup> Advanced Materials for Energy-Water Systems (AMEWS) Energy Frontier Research Center, Argonne National Laboratory, Lemont, IL 60439, USA

of precursor adsorbs on the substrate surface to subsequently react with the second one, and between each pulse a purge step is performed to remove the excess precursors.<sup>19</sup> ALD can form a conformal and tunable coating on substrates with diverse materials, morphologies, and size. ALD has found technological maturity in semiconductor device fabrication, and in research environments it is applied for a wide range of applications. Recently, membrane interface engineering has emerged as an exciting additional opportunity. ALD has three major advantages compared with traditional methods. Firstly, ALD is a largely substrate-independent process that can be directly conducted even on recognized low-energy surfaces such as PTFE (the nucleation mechanisms may be different for surfaces with different chemistries). Secondly, ALD creates a conformal coating even on highly tortuous substrates such as membranes, which not only retains the original pore structure of the membrane but also achieves nearly 100% coverage. This combination of attributes is important for catalytic or adsorptive membranes requiring high active area. Lastly, the coating thickness can be precisely and continuously tuned within a wide range from nanometers to micrometers.

Sequential infiltration synthesis (SIS), another interface engineering method,<sup>20–24</sup> is derived from ALD but is a qualitatively different process—and it, too, has demonstrated promise in tailoring membrane properties.<sup>25</sup> In SIS, the integrated exposure to the alternating vapor precursors is orders of magnitude larger than in ALD. This larger exposure allows the precursors to diffuse into polymer substrates rather than simply decorating the surface (Fig. 1, bottom). If the polymer has sites that will bind the first precursor, either by functional groups designed into the polymer itself or through defects/impurities, inorganic material can be grown within the near-surface of the substrate in a self-limited fashion. The kinetics of SIS are more complex than those of ALD because of the added aspect of in- and out-diffusion of precursors and reaction products, so process design becomes more important. Because the inorganic material is grown within, rather than on, the substrate, pore constriction is minimized while still allowing for manipulation of the physicochemical properties of the interface.

Despite these advantages of ALD in membrane interface engineering, research in this field is still in its infancy. Much remains to be learned, and there are undoubtedly opportunities not even yet envisioned for application of ALD and/or SIS in membrane science and engineering. ALD provides an ideal platform to investigate the relationship between membrane surface properties and membrane performance, and a powerful tool to reveal the interacting mechanisms between membrane surfaces and filtrating media. In this minireview, we summarize the recent advances in ALD-based membrane interface engineering. We categorize the literature into three sections categorized by the roles ALD plays in these applications.

## 2. ALD for membrane interface modification and functionalization

### 2.1 Direct surface modification

**Hydrophilization** One of the most important targets for membrane interface engineering is control over the wettability of the membrane surface. The challenge lies in the hydrophilization of membranes made of low-surface-energy materials such as PTFE and PP. These materials have non-polar hydrophobic surfaces that are chemically inert. ALD provides a promising hydrophilization strategy for these materials as it enables conformal coating with a hydrophilic material in spite of the non-reactive surface of the underlying membrane. For example, PTFE membranes can be directly modified with Al<sub>2</sub>O<sub>3</sub> through ALD without any pre-treatment (Fig. 2a).<sup>26</sup> The underlying mechanisms of Al<sub>2</sub>O<sub>3</sub> deposition are different for the inert PTFE surface compared to other membranes with polar surfaces. In the case of inert PTFE surfaces, discrete nanoparticles nucleate during the initial stages of ALD because of the dearth of active binding sites. With additional cycles, the nucleated nanoparticles proceed to grow by normal ALD into large clusters and eventually coalesce into a continuous coating. As a result, more than 300 ALD cycles are needed to realize the hydrophobic-to-hydrophilic transition of the membrane surface. A uniform and conformal coating with fewer ALD cycles can be achieved by activating the inert membrane surface to induce rapid nucleation. Xu et al. pre-treated PTFE membranes with short-time, low-power air plasma and then deposited TiO<sub>2</sub> on them (Fig. 2b).<sup>27</sup> The resulting membrane surface showed high uniformity and was rendered hydrophilic with only 100 ALD cycles. ALD on PP membranes is similar to ALD on PTFE. Both plasma<sup>28</sup> and nitric acid activation<sup>29</sup> have been demonstrated to promote the deposition process in this system.

Applications of these hydrophilized membranes include anti-fouling surfaces, oil/water separations, and Li-ion battery separators, among others. Nikkola et al. applied ALD of Al<sub>2</sub>O<sub>3</sub> on commercial nanofiltration (NF) and reverse osmosis (RO) membranes to improve the anti-biofouling property of the membranes.<sup>30</sup> Bacterial adhesion was slightly alleviated in membranes with thin ALD coatings due to the promoted hydrophilicity of the surface. Increased numbers of cycles and deposition at higher temperatures led to surprisingly large water contact angle increase, which might be ascribed to residual Al-CH<sub>3</sub> groups from the trimethylaluminum precursor. Juholin et al. deposited ZnO on commercial NF membranes for mining wastewater treatment and found both flux and anti-fouling performance to be improved.<sup>31</sup> To investigate the anti-fouling performance of different ALD oxide coatings, Li et al. compared the static adsorption of protein-polysaccharide hybrids on ZnO-, Al<sub>2</sub>O<sub>3</sub>-, and TiO<sub>2</sub>-coated PVDF membranes.<sup>32</sup> Each oxide showed improved performance over the nascent membrane, and the ZnO-coated membrane showed the lowest adsorption to both bovine serum albumin (BSA) and sodium alginate (SA). TiO<sub>2</sub>-coated membranes were more easily fouled by SA, while Al<sub>2</sub>O<sub>3</sub>-coated ones showed poor resistance to BSA. The specific interactions between particular foulants and particular metal oxide surfaces dictate how readily adhesion and fouling can occur.

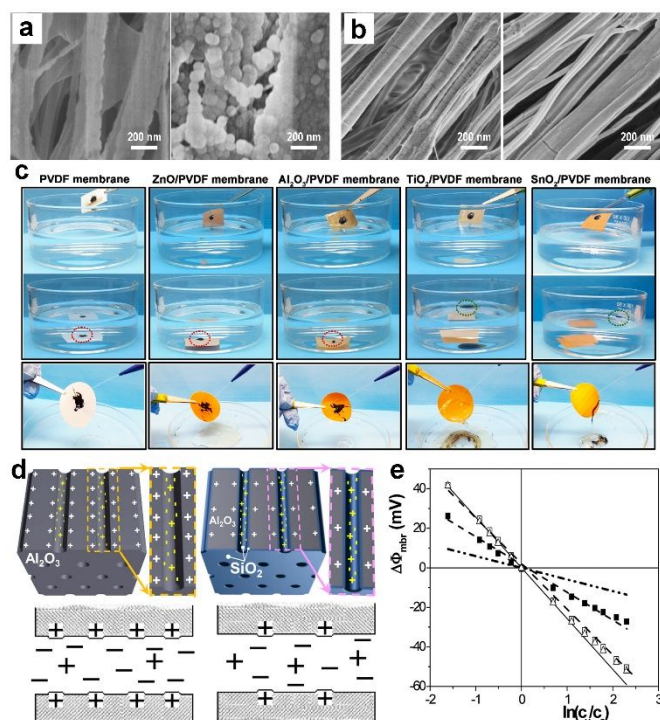


**Figure 2.** SEM images of a) nascent and  $\text{Al}_2\text{O}_3$ -coated (300 ALD cycles) PTFE membranes, and b) nascent and  $\text{TiO}_2$ -coated (300 ALD cycles) PTFE membrane pre-treated by air plasma. Reprinted with permission from ref.26 and 27. Copyright 2012, 2013, Elsevier. c) Anti-crude-oil performance of membranes coated with different oxides by ALD. Reprinted with permission from ref.36. Copyright 2018, ACS. d) Scheme of surface charges on AAO and  $\text{SiO}_2$ -coated AAO membranes. e) Membrane potential versus NaCl solution concentration ratio.  $\square$  and  $\Delta$  represent the nascent and  $\text{Al}_2\text{O}_3$ -coated membrane, while  $\blacksquare$  represents the  $\text{SiO}_2$ -coated membrane. Reprinted with permission from ref.39. Copyright 2013, ACS.

Recently, membranes coated with minerals have attracted interest for oil/water separations because of their rigid hierarchical structure and abundant hydrophilic surface moieties.<sup>33–35</sup> Our recent research investigated the anti-crude oil performance of membranes coated with different oxides by ALD (**Fig. 2c**).<sup>36</sup>  $\text{SnO}_2$ - and  $\text{TiO}_2$ -coated membranes provided much better crude oil protection than  $\text{Al}_2\text{O}_3$ - and  $\text{ZnO}$ -coated membranes. Molecular dynamic simulations revealed that the hydration layers on  $\text{SnO}_2$  and  $\text{TiO}_2$  surfaces are particularly tight and dense in a neutral aqueous environment, enabling facile release of the crude oil from the oxide surface under water.

ALD-modified membranes are also compelling candidates for the separator of lithium-ion batteries. The separators serve as a physical barrier between anode and cathode to avoid short circuits. Commercial separators made of polyolefin generally suffer from poor wettability to the electrolyte and undesired thermal shrinkage under high operation temperature, both of which can be addressed by ALD. Oxide coatings can increase the membrane surface wettability for higher electrolyte uptake, facilitating ion transport across the separator. The rigid inorganic coating can also stabilize the soft polymeric skeleton from harsh external environments like high temperature. Chen et al. coated polyethylene separators with  $\text{TiO}_2$  through ALD.<sup>37</sup> Both surface wettability and thermal stability were

significantly improved, and superior battery performance was achieved.

**Surface charge regulation** Beyond enhancing membrane surface wettability, ALD can be used to engineer membrane surface charges via the different isoelectric points of various metal oxides. Ion transport through nano-channels can be regulated by channel diameter and surface charge, both of which can be tailored by ALD through the number of ALD cycles employed and the choice of material deposited. It is worth mentioning that surface charge effects become significant when the channel dimension approaches nearly double the Debye length, at which scale the ion transport is governed by the electric double layer.<sup>38</sup> Romero et al. fabricated a series of anodic aluminum oxide (AAO) membranes of varied pore size through anodization and modified the inner channels with  $\text{SiO}_2$  by ALD (**Fig. 2d**).<sup>39</sup> The  $\text{Al}_2\text{O}_3$  membrane is positively charged while the  $\text{SiO}_2$  coating is negatively charged in neutral pH. Therefore, the  $\text{SiO}_2$  coating can notably reduce the effective fixed charge and alleviate the coulombic barrier effect to cation transport (**Fig. 2e**). Other metal oxides were investigated in a follow-up study, further demonstrating the wide materials library available in ALD for effective fixed charge engineering.<sup>40</sup> This library extends beyond metal oxides to other materials with high surface charge. For example Matthieu et al. grew boron nitride (BN) on AAO membranes by using  $\text{BBr}_3$  and  $\text{NH}_3$  as ALD precursors.<sup>41</sup> The highly charged surface dramatically hinders ionic transport across the membrane beyond simple pore-size sieving. Conductivity through the membrane is in the same order of magnitude for NaCl solutions with concentration ranging from  $10^{-4}$  to  $1 \text{ mol} \cdot \text{L}^{-1}$ , which shows weak concentration dependence as the result of the high charge density of the BN surface.<sup>42</sup>

**Functionalization** Due to their highly porous structures and large surface areas, membrane materials are ideal supports for catalysts and adsorbents. Both adsorption and catalytic processes occur at the interface, so high surface coverage of functional materials has beneficial impact on membrane performance. Compared with other functionalization strategies, such as blending or post-grafting, ALD can conformally modify the membrane surface without significantly changing the underlying porous structure. Semiconducting catalysts, such as  $\text{TiO}_2$  and  $\text{ZnO}$ , are obvious choices for photocatalytic applications. Chen et al. deposited  $\text{TiO}_2$  followed by Pt onto AAO membranes.<sup>43</sup> Both annealed  $\text{TiO}_2$ -coated and Pt/ $\text{TiO}_2$ -coated membranes exhibited photocatalytic activity to degrade methyl blue under UV light. However,  $\text{TiO}_2$  catalysts show limited activity under visible light because of the wide band gap, and the requirement of UV light increases costs and limits real-world applications. In an effort to overcome this limitation, Li et al. deposited  $\text{TiO}_2$  and  $\text{ZnO}$  alternatively to fabricate a hetero-structured catalytic layer on PVDF membranes. The catalytic activity in the visible light region was enhanced because the photo-generated electron–hole pairs could transport between  $\text{TiO}_2$  and  $\text{ZnO}$  for effective charge carrier separation.<sup>44</sup> The optimal  $\text{TiO}_2/\text{ZnO}$  ratio in their study was 1:3. Another approach to enabling visible-light-driven photocatalysis is to dope  $\text{TiO}_2$  to shift its band-edge into the visible range. In our previous work, we fabricated N-doped  $\text{TiO}_2$  coatings on ceramic membranes by employing  $\text{TiCl}_4$  and  $\text{H}_2\text{O}$  as ALD precursors with intermittent pulses of  $\text{NH}_3 \cdot \text{H}_2\text{O}$  (**Fig. 3a**).<sup>45</sup> High temperature ( $>375 \text{ }^\circ\text{C}$ ) was

needed to initiate the reactions to allow for substitutional doping of O sites with N. The N-doped TiO<sub>2</sub> coated membranes displayed excellent photocatalytic activity to degrade methyl orange under simulated sunlight as well as enhanced hydrophilicity (Fig. 3b).

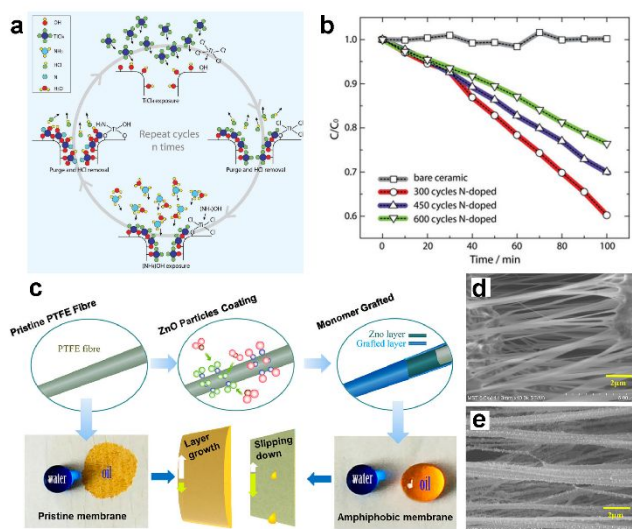


**Figure 3.** a) Scheme of ALD process for N-doped TiO<sub>2</sub> coated membrane. b) Visible light photocatalytic activity of N-doped TiO<sub>2</sub> coated membrane for degrading methyl orange. Reprinted with permission from ref.45. Copyright 2017, Wiley. c) Fabrication of amphiphobic fibrous membrane by ZnO ALD and fluorination. d) and e) are nascent and ZnO-coated PTFE membranes, respectively. Reprinted with permission from ref.52. Copyright 2016, ACS.

Affinity interactions can also be imparted to membranes using ALD strategies, offering a new route to designer adsorbents. Some ALD coatings exhibit strong adsorption activity to organic pollutants in water. For example, ZnO-coated membranes can adsorb both positively and negatively charged dyes through electrostatic, hydrogen bond, and chelation interactions.<sup>46</sup> Moreover, ZnO applied on AAO membranes has also shown anti-bacterial activity.<sup>47</sup>

## 2.2 Intermediate layer for post-functionalization

While in many applications the ALD coating serves as the active layer itself, ALD coatings can also serve as an intermediate layer for post-functionalization. Al<sub>2</sub>O<sub>3</sub> can be grown on the entire interior pore surfaces of highly tortuous membranes by SIS or ALD, leaving a hydroxyl-terminated surface that can accommodate a wide range of grafting macromolecules.<sup>48</sup> For example, Al<sub>2</sub>O<sub>3</sub>-coated membrane and sponge surfaces were rendered hydrophobic after grafting fluoric or alkyl silanes,<sup>49–51</sup> and such membranes can be applied in oil/water separation. ZnO is one of the most widely used intermediate layers for post-modification because it can act as a seed layer for ZnO nanorod growth, which can not only change the surface chemistry but also introduce functionality associated with hierarchical structures.<sup>52–54</sup> For example, Wang's group fabricated a ZnO layer on polyethylene terephthalate (PET) nonwoven fabric surfaces, and subsequently grew ZnO nanorods by a hydrothermal process.<sup>53</sup> The resulting structure of arrayed nanorods introduced a new function: to reserve liquids within structures for switchable oil/water separation. When the fabric was pre-wetted with water, it exhibited underwater

oleophobicity, allowing water permeation and rejecting oil. If the fabric was instead initially wetted with oil, the performance was reversed. In other work from the Wang group, the ZnO nanorods were decorated with Ag nanoparticles and then applied as an anti-bacterial air filter.<sup>54</sup> Utilizing the discrete nanoparticle deposition by ALD on inert polymer surfaces, Wang's group used PTFE membranes as a substrate for the growth of isolated ZnO nuclei. The nanoscale roughness associated with this deposit, coupled with subsequent surface fluorination, enabled an amphiphobic device that showed effective filtration of organic aerosols (Fig. 3c-e).<sup>52</sup>

## 3. ALD for membrane structure regulation

### 3.1 Tuning membrane pores

The layer-by-layer nature of ALD enables researchers to control the morphology of membranes via constriction of pore size. As a universal strategy, ALD can be applied on both polymer<sup>55</sup> and ceramic membranes,<sup>56</sup> with straight<sup>57,58</sup> or tortuous<sup>59</sup> pore structures. For example, Wang's group deposited Al<sub>2</sub>O<sub>3</sub> on ZrO<sub>2</sub> ceramic membranes<sup>56</sup> and track-etched polycarbonate membranes to modify the membrane pore size.<sup>57</sup> The rejection to BSA increased while the permeate flux decreased with increasing number of ALD cycles. When the underlying material is different than the ALD-deposited surface, the effects of pore size constriction must be decoupled from the change in surface wettability and chemistry. The same group coated TiO<sub>2</sub> on PVDF membranes with increasing cycle numbers and observed a trade-off effect. At low cycle numbers, the pure water flux was increased due to the promoted hydrophilicity of TiO<sub>2</sub> over PVDF. However, at approximately 120 cycles, the constriction of the pore dimension outweighed the enhancement of the TiO<sub>2</sub> surface and the flux began to decline.<sup>55</sup> Similar phenomena were reported by Lee et al.<sup>45</sup>

At sufficient thickness, inorganic ALD coatings can become brittle materials and can compromise the mechanical properties of the resultant membrane. To address this problem, Wang's group attempted to deposit polyimide on polyethersulfone membrane surface for pore size adjustment.<sup>59,60</sup> Pyromellitic dianhydride and ethylenediamine were used as the precursors through a variant of ALD known as molecular layer deposition (MLD). The polyimide coating could be further crosslinked by ethylenediamine for improved hydrophilicity and stability.<sup>60</sup> The flexibility of the membrane was retained after MLD. Moreover, the thermal stability of the membrane could be significantly enhanced by polyimide coating because of its high-temperature resistance.

### 3.2 Selective layer construction

The discussion so far has detailed ALD-modifications to microfiltration and ultrafiltration membranes that achieve separations based on size-selective sieving. Another class of membranes composed of a dense skin layer and a porous support layer are known as thin film composite (TFC) membranes, in which the separation mechanism is based on diffusion across a dense layer. Such membranes find wide use in nanofiltration, reverse osmosis,

forward osmosis, and gas separation. Researchers have used ALD to construct TFC membranes by completely sealing up pores via layer-by-layer constriction. A small-pore substrate, as well as brief pulses and exposure durations are normally applied to avoid undesired defects and locate the deposition at the near-surface region. For example, Tran et al. deposited a thin layer of TiO<sub>2</sub> on the top surface of an Al<sub>2</sub>O<sub>3</sub> ceramic membrane.<sup>61</sup> They firstly dip-coated a boehmite sol on the substrate surface to reduce the pore size (forming a  $\gamma$ -Al<sub>2</sub>O<sub>3</sub> top layer), and subsequently used TiO<sub>2</sub> ALD to seal this material into a dense layer. The obtained membrane showed a separation factor of 5.8 for H<sub>2</sub> in a H<sub>2</sub>/CO<sub>2</sub> mixture at 448 K, competitive with other inorganic gas separation membranes. ALD-based TFC membranes have also been applied in aqueous separations. Song et al. deposited titanocene, using TiCl<sub>4</sub> and ethylene glycol as the precursors, onto AAO membranes with asymmetric pore structures. Calcination of the titanocene at 400 °C to remove the organic constituents produced a dense TiO<sub>2</sub> layer.<sup>62</sup> The prepared membrane could not reject salts effectively, but was extremely effective at rejecting dyes like methyl blue. Chen et al. conducted the same process on the lumen surface of an Al<sub>2</sub>O<sub>3</sub>/TiO<sub>2</sub> ceramic tubular membrane, which is more suitable for practical separation processes.<sup>63</sup> The membrane flux decreased from  $\sim 100 \text{ L m}^{-2} \text{ h}^{-1} \text{ bar}^{-1}$  to  $45 \text{ L m}^{-2} \text{ h}^{-1} \text{ bar}^{-1}$  while the molecular weight cut-off was reduced from  $\sim 7200 \text{ Da}$  to  $\sim 2600 \text{ Da}$ . Direct deposition of TiO<sub>2</sub> on an ultrafiltration membrane could also be used narrow the pore size,<sup>64,65</sup> but the TFC membranes formed by ALD showed poor rejection to divalent ions. Again, most of these membranes were best used to remove larger organic dyes because of the intrinsic micropores in inorganic ALD coatings.

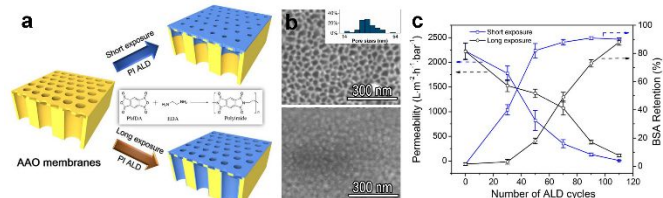


**Figure 4.** a) Scheme of polyimide (PI) deposition on AAO membranes with different exposure time. b) SEM images of nascent and PI-coated membranes with 120 ALD cycles. c) Permeability and rejection of BSA solution of membranes with short and long exposure time. Reprinted with permission from ref.66. Copyright 2017, Elsevier.

Polymeric TFC membranes are most commonly fabricated through an interfacial polymerization process. As mentioned in section 3.1, Wang's group developed a novel polyimide TFC membrane on AAO substrates based on ALD (or, more precisely, MLD).<sup>66</sup> By applying a short-exposure duration, the deposition process could be limited to the top surface of the substrate, rather than the whole membrane, and finally achieve a TFC membrane (Fig. 4a-b). The TFC membrane showed much higher rejection with increasing ALD cycles compared with the PI-modified membrane (Fig. 4c).

## 4. ALD for advanced membranes and membrane processes

### 4.1 Janus membranes

The emerging concept of Janus membranes has attracted widespread interest owing to their broad potential in membrane processes such as emulsification/demulsification,<sup>67</sup> membrane distillation,<sup>68</sup> and aeration,<sup>69</sup> to name a few. The term "Janus membrane" refers to a membrane where the two surfaces have opposing properties, such as hydrophilicity/hydrophobicity, or positive charges/negative charges.<sup>70,71</sup> In general, Janus structures can be achieved by integrating two distinct layers or by conducting asymmetric modifications to an extant membrane. Though ALD has generally been used as a conformal technique in membranes, control over the diffusion of the precursor vapors through highly tortuous and high-aspect-ratio porous materials can enable gradient coatings leading to Janus membranes. The control over the precursor dosing and total number of cycles allows for precise control of the modification gradient from one side of the membrane to the other. Our group performed diffusion-controlled ALD of Al<sub>2</sub>O<sub>3</sub> on hydrophobic PP microfiltration membranes (Fig. 5a).<sup>72</sup> Only one surface of the membrane was exposed to the precursors, and the Knudsen flow and low nucleation rate of the process yielded hydrophilicity gradients that could be arbitrarily tuned (Fig. 5b). This approach to fabricating Janus membranes offers a level of control unachievable using most other methods.

Alternatively, depth-limited physicochemical masking of the pore surface can bypass the need for diffusion-based control in ALD Janus membrane fabrication. Fu et al., for example, applied ALD as a surface modification strategy to fabricate Janus membranes for CO<sub>2</sub> separation.<sup>73</sup> A porous AAO membrane was modified with hydrophobic silane via ALD followed by O<sub>2</sub> plasma treatment on the top surface, which oxidized away the silane to a certain depth rendering the exposed Al<sub>2</sub>O<sub>3</sub> surface active for a subsequent ALD coating.

### 4.2 Isoporous membranes templated by block copolymers

Block copolymers (BCPs) are materials that self-assemble into chemically distinct nanoscale patterns (spheres, lamellae, cylinders, etc.) with dimensions dictated by molecular weight and penalty of mixing between blocks. In the context of membranes, BCPs can assemble into thin films with bicontinuous sponge-like structures<sup>74,75</sup> or with straight cylindrical domains,<sup>76</sup> serving as a template for membrane fabrication. While selective block etching and selective solvent swelling have been used to transform these nanoscale domains into pores to yield a polymer membrane, ALD and its variant SIS can be used to transform one block into a metal oxide. Nealey's group conducted SIS of Al<sub>2</sub>O<sub>3</sub> on cylinder-forming poly(styrene-*b*-methyl methacrylate) (PS-*b*-PMMA) films to fabricate isoporous Al<sub>2</sub>O<sub>3</sub> ultrafiltration membranes (Fig. 5c).<sup>76</sup> In the BCP film, the PS block forms the cylinder phase, and the precursors can solely bind with the (matrix) PMMA domains because of the formation of a complex with the PMMA carbonyl moieties.<sup>62</sup> Straight pores were obtained by removing the unmodified PS blocks by O<sub>2</sub> reactive ion etching. The PMMA that is swollen with metal oxide by the SIS is also removed in this process, leaving behind Al<sub>2</sub>O<sub>3</sub> that directly matches the original PMMA

template. The  $\text{Al}_2\text{O}_3$ -infiltrated skeleton could not only adjust the membrane pore size for various separation demands, but also increase the hydrophilicity and stability of the membrane (Fig. 5d). The narrow pore distribution of the BCP-templated membranes exhibited much higher selectivity, in particular to proteins with similar size. The separation selectivity is closely related to the environment pH, and the maximum protein flux is achieved at the isoelectric point of the protein (Fig. 5e).

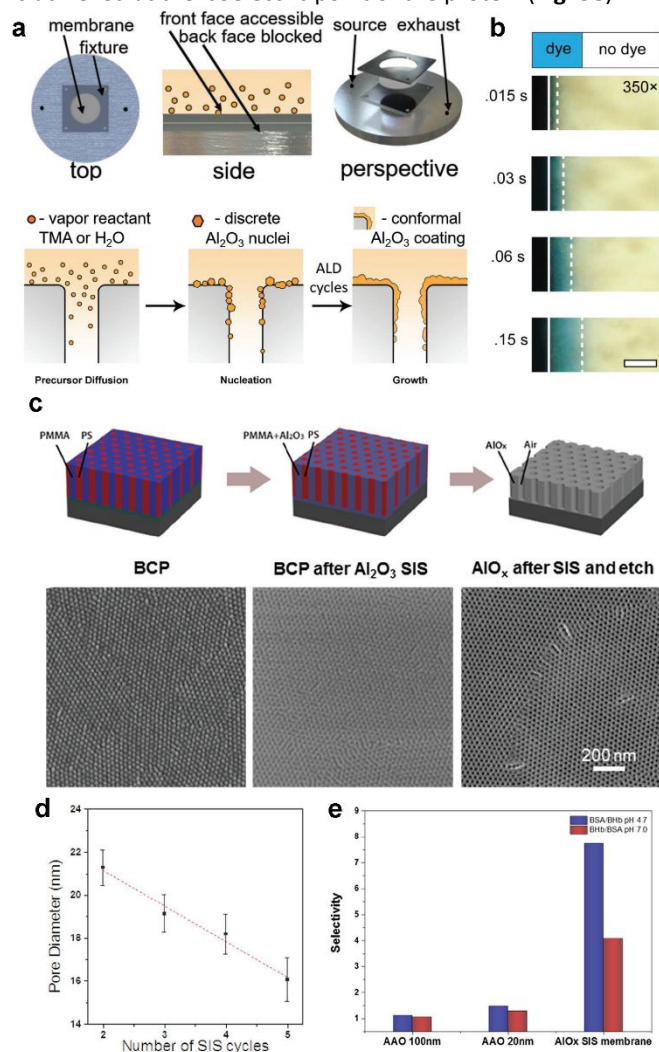


**Figure 5.** a) Fabrication process and mechanism of Janus membrane by diffusion-controlled ALD. b) Thickness control of the Janus membranes by ALD exposure time. Reprinted with permission from ref.72. Copyright 2018, Wiley. c) Fabrication of block copolymer (BCP) templated  $\text{Al}_2\text{O}_3$  isoporous membrane by SIS and corresponding SEM images. d) Pore size of BCP-templated membranes decreases with SIS cycles. e) Selectivity of BSA/BHb by nascent AAO and BCP-templated membranes. Reprinted with permission from ref.76. Copyright 2018, Wiley.

## 5. Conclusion and perspective

In this minireview, we present the recent advances of ALD, a well-known nanofabrication technology, as applied to membranes and membrane processes. ALD enables the deposition of atomically precise conformal layers of a wide variety of materials (inorganic

metal oxides, metals, etc.), and initial studies have shown that ALD can completely and conformally cover the inner pore structure of highly tortuous polymer membranes. Introducing an inorganic conformal coating allows researchers to extend the functionality of membranes in several domains: 1) The new surface chemistry can improve hydrophilicity and sometimes introduce new functions like catalytic and adsorptive activity. 2) The inorganic coating can act as a platform for functional molecule grafting via silane-coupling or other chemistries. 3) The layer-by-layer growth of ALD can allow for precision pore-size tailoring. 4) By controlling the diffusion of precursors through ALD parameters, the deposition can be located at the membrane top surface or inner structure, enabling the fabrication of TFC membranes and Janus membranes. While the literature has a growing number of reports in this field, much remains to be learned regarding the use of ALD and related methods (SIS, MLD, etc.) in interface engineering for high-performance and multi-functional membrane materials.

Despite the many advantages of ALD, this method still has some drawbacks when applied to membrane surface modification, which at the same time represent potential opportunities in future research. For example, ALD of oxides may compromise the mechanical strength of polymer membranes because of the intrinsic rigidity of inorganics. This issue may be overcome by applying organic or organic-inorganic hybrid coatings. Another challenge is that many ALD coatings are formed only at high temperature, which may exceed the melting point of polymers used in commercial membranes. The demand for more applicable materials will drive the development of low-temperature ALD processes.

The capacity of ALD to integrate materials is arguably undervalued. The conformal coating can serve as an adhesive to integrate, for example, nanomaterials with membranes. In our recent research, we applied ALD on calligraphy-ink-coated membranes and other substrates for solar steam generation,<sup>77</sup> and the ALD coating could stabilize the ink-coating against re-dispersion into the surrounding water. Beyond the applications discussed in this minireview, organic-inorganic composite membranes may also find uses in membrane distillation, membrane contactors, enzyme immobilization for membrane bio-reactors, and many other applications.<sup>16</sup> Most such applications require high surface coverage of inorganics, which can be easily achieved by ALD. Although the standard layer-by-layer ALD growth has been shown to improve membranes, moving forward researchers are increasingly exploring processes that deviate from this typical growth pattern. SIS, for example, has emerged as a technique to replicate the membrane structure with a hybrid polymer-inorganic material, rather than just a coated polymer. Diffusion-limited techniques, too, offer enticing possibilities such as enabling Janus membranes with new functionality. These types of processes will facilitate interface engineering that simpler ALD cannot achieve. Another opportunity lies in ALD on hollow fiber membranes. This class of membranes is more common in industrial applications than flat-sheet form factors. However, few studies have been conducted to date. A recent paper reported deposition of  $\text{Al}_2\text{O}_3$  on PP hollow fibers for surface hydrophilization, and an unexpected promotion on elongation at break was observed after over 100 cycles of deposition.<sup>78</sup> More studies devoted to ALD on hollow fiber membranes are needed, in particular for achieving uniform selective

layer construction and understanding this process. Lastly, compared with other strategies to fabricate Janus membranes, diffusion-controlled ALD can precisely tune the ratio and gradient of the two properties in a Janus structure, which provides a useful tool to investigate the unusual transport mechanisms of Janus membranes as well as regulate their performance. Given the diverse library of substrate materials combined with the many inorganic species that can be deposited by ALD and related methods, coupled further with the potential for post-functionalization and other process innovations, the opportunities for advances in membrane science and engineering are virtually limitless.

## Conflicts of interest

There are no conflicts to declare.

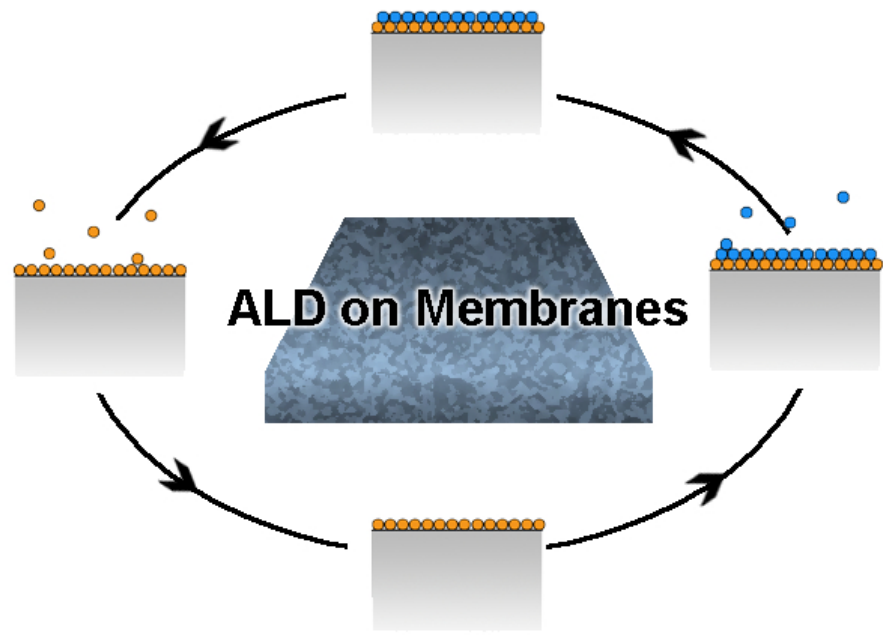
## Acknowledgements

This work was supported as part of the Advanced Materials for Energy-Water Systems (AMEWS) Center, an Energy Frontier Research Center funded by the U.S. Department of Energy, Office of Science, Basic Energy Sciences. H.-C. Yang acknowledges financial support from the Hundred Talents Program of Sun Yat-Sen University.

## Notes and references

- 1 A. Lee, J. W. Elam and S. B. Darling, *Environ. Sci. Water Res. Technol.*, 2016, **2**, 17–42.
- 2 J. R. Werber, C. O. Osuji and M. Elimelech, *Nat. Rev. Mater.*, DOI:10.1038/natrevmats.2016.18.
- 3 B. E. Logan and M. Elimelech, *Nature*, 2012, **488**, 313–319.
- 4 S. B. Darling, *J. Appl. Phys.*, DOI:10.1063/1.5040110.
- 5 E. Karatairi and S. B. Darling, *MRS Bull.*, 2018, **43**, 404–405.
- 6 K. S. Kim, K. H. Lee, K. Cho and C. E. Park, *J. Memb. Sci.*, 2002, **199**, 135–145.
- 7 K. R. Kull, M. L. Steen and E. R. Fisher, *J. Memb. Sci.*, 2005, **246**, 203–215.
- 8 C.-H. Zhang, F.-I. Yang, W.-J. Wang and B. Chen, *Sep. Purif. Technol.*, 2008, **61**, 276–286.
- 9 M. Ulbricht and G. Belfort, *J. Memb. Sci.*, 1996, **111**, 193–215.
- 10 D. S. Wavhal and E. R. Fisher, *J. Memb. Sci.*, 2002, **209**, 255–269.
- 11 D. M. Dotzauer, J. Dai, L. Sun and M. L. Bruening, *Nano Lett.*, 2006, **6**, 2268–2272.
- 12 M. L. Bruening, D. M. Dotzauer, P. Jain, L. Ouyang and G. L. Baker, *Langmuir*, 2008, **24**, 7663–7673.
- 13 H.-C. Yang, J. Luo, Y. Lv, P. Shen and Z.-K. Xu, *J. Memb. Sci.*, 2015, **483**, 42–59.
- 14 H.-C. Yang, R. Z. Waldman, M.-B. Wu, J. Hou, L. Chen, S. B. Darling and Z.-K. Xu, *Adv. Funct. Mater.*, 2018, **28**, 1705327.
- 15 D. Rana and T. Matsuura, *Chem. Rev.*, 2010, **110**, 2448–2471.
- 16 H.-C. Yang, J. Hou, V. Chen and Z.-K. Xu, *J. Mater. Chem. A*, 2016, **4**, 9716–9729.
- 17 S. M. George, *Chem. Rev.*, 2010, **110**, 111–131.
- 18 M. Leskelä and M. Ritala, *Angew. Chemie - Int. Ed.*, 2003, **42**, 5548–5554.
- 19 M. Leskelä and M. Ritala, *Thin Solid Films*, 2002, **409**, 138–146.
- 20 Q. Peng, Y.-C. Tseng, S. B. Darling and J. W. Elam, *ACS Nano*, 2011, **5**, 4600–4606.
- 21 Y.-C. Tseng, Q. Peng, L. E. Ocola, D. A. Czaplewski, J. W. Elam and S. B. Darling, *J. Mater. Chem.*, 2011, **21**, 11722–11725.
- 22 Y.-C. Tseng, Q. Peng, L. E. Ocola, J. W. Elam and S. B. Darling, *J. Phys. Chem. C*, 2011, **115**, 17725–17729.
- 23 M. Biswas, J. A. Libera, S. B. Darling and J. W. Elam, *Chem. Mater.*, 2014, **26**, 6135–6141.
- 24 Y. Yu, Z. Li, Y. Wang, S. Gong and X. Wang, *Adv. Mater.*, 2015, **27**, 4938–4944.
- 25 M. Ramanathan, Y. C. Tseng, K. Ariga and S. B. Darling, *J. Mater. Chem. C*, 2013, **1**, 2080–2091.
- 26 Q. Xu, Y. Yang, X. Wang, Z. Wang, W. Jin, J. Huang and Y. Wang, *J. Memb. Sci.*, 2012, **415–416**, 435–443.
- 27 Q. Xu, Y. Yang, J. Yang, X. Wang, Z. Wang and Y. Wang, *J. Memb. Sci.*, 2013, **443**, 62–68.
- 28 Q. Xu, J. Yang, J. Dai, Y. Yang, X. Chen and Y. Wang, *J. Memb. Sci.*, 2013, **448**, 215–222.
- 29 H. Chen, L. Kong and Y. Wang, *J. Memb. Sci.*, 2015, **487**, 109–116.
- 30 J. Nikkola, J. Sievänen, M. Raulio, J. Wei, J. Vuorinen and C. Y. Tang, *J. Memb. Sci.*, 2014, **450**, 174–180.
- 31 P. Juholin, M. L. Kääriäinen, M. Riihimäki, R. Sliz, J. L. Aguirre, M. Piriälä, T. Fabritius, D. Cameron and R. L. Keiski, *Sep. Purif. Technol.*, 2018, **192**, 69–77.
- 32 N. Li, Y. Tian, J. Zhao, J. Zhang, L. Kong, J. Zhang and W. Zuo, *J. Memb. Sci.*, 2018, **548**, 470–480.
- 33 C. Zhang, H.-C. Yang, L.-S. Wan, H.-Q. Liang, H. Li and Z.-K. Xu, *ACS Appl. Mater. Interfaces*, 2015, **7**, 11567–11574.
- 34 H. C. Yang, J. K. Pi, K. J. Liao, H. Huang, Q. Y. Wu, X. J. Huang and Z. K. Xu, *ACS Appl. Mater. Interfaces*, 2014, **6**, 12566–12572.
- 35 H.-C. Yang, Y.-F. Chen, C. Ye, Y.-N. Jin, H. Li and Z.-K. Xu, *Chem. Commun.*, 2015, **51**, 12779–12782.
- 36 H.-C. Yang, Y. Xie, H. Chan, B. Narayanan, L. Chen, R. Z. Waldman, S. K. R. S. Sankaranarayanan, J. W. Elam and S. B. Darling, *ACS Nano*, 2018, acsnano.8b04632.
- 37 H. Chen, Q. Lin, Q. Xu, Y. Yang, Z. Shao and Y. Wang, *J. Memb. Sci.*, 2014, **458**, 217–224.
- 38 X. Huang, X. Y. Kong, L. Wen and L. Jiang, *Adv. Funct. Mater.*, DOI:10.1002/adfm.201801079.
- 39 V. Romero, V. Vega, J. García, R. Zierold, K. Nielsch, V. M. Prida, B. Hernando and J. Benavente, *ACS Appl. Mater. Interfaces*, 2013, **5**, 3556–3564.
- 40 V. Vega, L. Gelde, A. S. González, V. M. Prida, B. Hernando and J. Benavente, *J. Ind. Eng. Chem.*, 2017, **52**, 66–72.
- 41 M. Weber, B. Koonkaew, S. Balme, I. Utke, F. Picaud, I. Iatsunskyi, E. Coy, P. Miele and M. Bechelany, *ACS Appl. Mater. Interfaces*, 2017, **9**, 16669–16678.

- 42 A. Siria, P. Poncharal, A. L. Biance, R. Fulcrand, X. Blase, S. T. Purcell and L. Bocquet, *Nature*, 2013, **494**, 455–458.
- 43 H. S. Chen, P. H. Chen, S. H. Huang and T. P. Perng, *Chem. Commun.*, 2014, **50**, 4379–4382.
- 44 N. Li, Y. Tian, J. Zhang, Z. Sun, J. Zhao, J. Zhang and W. Zuo, *J. Memb. Sci.*, 2017, **528**, 359–368.
- 45 A. Lee, J. A. Libera, R. Z. Waldman, A. Ahmed, J. R. Avila, J. W. Elam and S. B. Darling, *Adv. Sustain. Syst.*, 2017, **1**, 1600041.
- 46 S. Xiong, L. Kong, Z. Zhong and Y. Wang, *AIChE J.*, 2016, **62**, 3982.
- 47 J. Feng, S. Xiong, Z. Wang, Z. Cui, S. P. Sun and Y. Wang, *J. Memb. Sci.*, 2018, **550**, 246–253.
- 48 R. Z. Waldman, D. Choudhury, D. J. Mandia, J. W. Elam, P. F. Nealey, A. B. F. Martinson and S. B. Darling, *Jom*, 2018, 1–12.
- 49 E. Barry, A. U. Mane, J. A. Libera, J. W. Elam and S. B. Darling, *J. Mater. Chem. A*, 2017, 2929–2935.
- 50 E. Barry, J. A. Libera, A. U. Mane, J. R. Avila, D. DeVitis, K. Van Dyke, J. W. Elam and S. B. Darling, *Environ. Sci. Water Res. Technol.*, 2018, **4**, 40–47.
- 51 L. Kong, Q. Wang, S. Xiong and Y. Wang, *Ind. Eng. Chem. Res.*, 2014, **53**, 16516–16522.
- 52 S. Feng, Z. Zhong, F. Zhang, Y. Wang and W. Xing, *ACS Appl. Mater. Interfaces*, 2016, **8**, 8773–8781.
- 53 S. Xiong, L. Kong, J. Huang, X. Chen and Y. Wang, *J. Memb. Sci.*, 2015, **493**, 478–485.
- 54 S. Feng, D. Li, Z. xian Low, Z. Liu, Z. Zhong, Y. Hu, Y. Wang and W. Xing, *J. Memb. Sci.*, 2017, **531**, 86–93.
- 55 Q. Wang, X. Wang, Z. Wang, J. Huang and Y. Wang, *J. Memb. Sci.*, 2013, **442**, 57–64.
- 56 F. Li, Y. Yang, Y. Fan, W. Xing and Y. Wang, *J. Memb. Sci.*, 2012, **397–398**, 17–23.
- 57 F. Li, L. Li, X. Liao and Y. Wang, *J. Memb. Sci.*, 2011, **385–386**, 1–9.
- 58 L. Velleman, G. Triani, P. J. Evans, J. G. Shapter and D. Losic, *Microporous Mesoporous Mater.*, 2009, **126**, 87–94.
- 59 T. Sheng, H. Chen, S. Xiong, X. Chen and Y. Wang, *AIChE J.*, 2014, **60**, 3614–3622.
- 60 T. Sheng, L. Kong and Y. Wang, *J. Memb. Sci.*, 2015, **486**, 161–168.
- 61 T. H. Y. Tran, W. G. Haije, V. Longo, W. M. M. Kessels and J. Schoonman, *J. Memb. Sci.*, 2011, **378**, 438–443.
- 62 Z. Song, M. Fathizadeh, Y. Huang, K. H. Chu, Y. Yoon, L. Wang, W. L. Xu and M. Yu, *J. Memb. Sci.*, 2016, **510**, 72–78.
- 63 H. Chen, X. Jia, M. Wei and Y. Wang, *J. Memb. Sci.*, 2017, **528**, 95–102.
- 64 H. Chen, S. Wu, X. Jia, S. Xiong and Y. Wang, *AIChE J.*, 2018, **64**, 2670–2678.
- 65 R. Shang, A. Goulas, C. Y. Tang, X. de Frias Serra, L. C. Rietveld and S. G. J. Heijman, *J. Memb. Sci.*, 2017, **528**, 163–170.
- 66 H. Wang, M. Wei, Z. Zhong and Y. Wang, *J. Memb. Sci.*, 2017, **535**, 56–62.
- 67 M. B. Wu, H. C. Yang, J. J. Wang, G. P. Wu and Z. K. Xu, *ACS Appl. Mater. Interfaces*, 2017, **9**, 5062–5066.
- 68 H. C. Yang, W. Zhong, J. Hou, V. Chen and Z. K. Xu, *J. Memb. Sci.*, 2017, **523**, 1–7.
- 69 H. C. Yang, J. Hou, L. S. Wan, V. Chen and Z. K. Xu, *Adv. Mater. Interfaces*, 2016, **3**, 1–5.
- 70 H. C. Yang, J. Hou, V. Chen and Z. K. Xu, *Angew. Chemie - Int. Ed.*, 2016, **55**, 13398–13407.
- 71 H. C. Yang, Y. Xie, J. Hou, A. K. Cheetham, V. Chen and S. B. Darling, *Adv. Mater.*, 2018, **33**, 1801495.
- 72 R. Z. Waldman, H. Yang, D. J. Mandia, P. F. Nealey, J. W. Elam and S. B. Darling, *Adv. Mater. Interfaces*, 2018, **5**, 1800658.
- 73 Y. Fu, Y.-B. Jiang, D. Dunphy, H. Xiong, E. Coker, S. Chou, H. Zhang, J. M. Vanegas, J. G. Croissant, J. L. Cecchi, S. B. Rempe and C. J. Brinker, *Nat. Commun.*, 2018, **9**, 990.
- 74 F. Li, X. Yao, Z. Wang, W. Xing, W. Jin, J. Huang and Y. Wang, *Nano Lett.*, 2012, **12**, 5033–5038.
- 75 L. Guo, Z. Zhong and Y. Wang, *Adv. Mater. Interfaces*, 2016, **3**, 1–9.
- 76 C. Zhou, T. Segal-Peretz, M. E. Oruc, H. S. Suh, G. Wu and P. F. Nealey, *Adv. Funct. Mater.*, 2017, **27**, 1701756.
- 77 H. Yang, Z. Chen, Y. Xie, J. Wang, J. W. Elam, W. Li and S. B. Darling, 2018, **1801252**, 1–7.
- 78 X. Jia, Z. Low, H. Chen, S. Xiong and Y. Wang, *Chinese J. Chem. Eng.*, 2018, **26**, 695–700.



56x41mm (300 x 300 DPI)